Structural plasticity of perisynaptic astrocyte processes involves ezrin and metabotropic glutamate receptors

Monique Lavialle[a], Georg Aumann[b], Enrico Anlauf[b], Felicitas Pröls[c], Monique Arpin[d], and Amin Derouiche[b,e,f,g,h,1]

[a]Institut National de la Recherche Agronomique, Unité de Nutrition et Régulation Lipidique des Fonctions Cérébrales 909, 78352 Jouy-en-Josas, France; [b]Institute of Anatomy, Technical University of Dresden, 01307 Dresden, Germany; [c]Institute of Anatomy I: Cellular Neurobiology, Universitätsklinikum Eppendorf, 20246 Hamburg, Germany; [d]Morphogenèse et Signalisation Cellulaires, Unité Mixte de Recherche 144, Centre National de la Recherche Scientifique/Institut Curie, 75248 Paris 5, France; [e]Institute for Anatomy and Cell Biology, University of Freiburg, 79104 Freiburg, Germany; [f]Institute of Cellular Neurosciences, University of Bonn, 53105 Bonn, Germany; [g]Institute of Anatomy II, University of Frankfurt, 60590 Frankfurt, Germany; and [h]Dr. Senckenbergisches, Chronomedizinisches Institut, University of Frankfurt, 60590 Frankfurt, Germany

Edited by Tomas G. M. Hökfelt, Karolinska Institutet, Stockholm, Sweden, and approved June 20, 2011 (received for review January 25, 2011)

The peripheral astrocyte process (PAP) preferentially associates with the synapse. The PAP, which is not found around every synapse, extends to or withdraws from it in an activity-dependent manner. Although the pre- and postsynaptic elements have been described in great molecular detail, relatively little is known about the PAP because of its difficult access for electrophysiology or light microscopy, as they are smaller than microscopic resolution. We investigated possible stimuli and mechanisms of PAP plasticity. Immunocytochemistry on rat brain sections demonstrates that the actin-binding protein ezrin and the metabotropic glutamate receptors (mGluRs) 3 and 5 are compartmentalized to the PAP but not to the GFAP-containing stem process. Further experiments applying ezrin siRNA or dominant-negative ezrin in primary astrocytes indicate that filopodia formation and motility require ezrin in the membrane/cytoskeleton bound (i.e., T567-phosphorylated) form. Glial processes around synapses in situ consistently display this ezrin form. Possible motility stimuli of perisynaptic glial processes were studied in culture, based on their similarity with filopodia. Glutamate and glutamate analogues reveal that rapid (5 min), glutamate-induced filopodia motility is mediated by mGluRs 3 and 5. Ultrastructurally, these mGluR subtypes were also localized in astrocytes in the rat hippocampus, preferentially in their fine PAPs. In vivo, changes in glutamatergic circadian activity in the hamster suprachiasmatic nucleus are accompanied by changes of ezrin immunoreactivity in the suprachiasmatic nucleus, in line with transmitter-induced perisynaptic glial motility. The data suggest that (*i*) ezrin is required for the structural plasticity of PAPs and (*ii*) mGluRs can stimulate PAP plasticity.

ERM proteins | suprachiasmatic nucleus | circadian regulation | actin cytoskeleton | deconvolution

Astrocytes act as a third partner in synaptic signal processing by responding to neurotransmitters and by releasing "gliotransmitters" (1, 2). Structurally, the astrocyte functions mainly through its peripheral processes, which constitute approximately 80% of the cell's membrane (3). These peripheral astrocyte processes (PAPs) are frequently extremely fine (<50 nm) and display an extreme surface-to-volume ratio. They are rarely studied in live tissue, as they are not directly accessible to electrophysiology, cannot be isolated for biochemistry, and are smaller than microscopic resolution. However, they also wrap synapses, but most studies on glia–synaptic interaction can only indiscriminately refer to them as the astrocyte. At the ultrastructural level, the PAPs, although abundant in the neuropil, specifically prefer contacting synapses and dendrites versus axons (4). The synaptic wrapping is highly dynamic (5–9) and also activity-dependent even in the context of physiological functions, such as motor learning, daily fluctuations of the circadian clock, lactation, parturition, or dehydration (10–15). Here, we asked two questions about the structural basis of glia–synaptic interaction: What is the stimulus for PAP plasticity, and what are the intracellular mechanisms accomplishing the motility and the formation of the PAP? We and others have shown that the membrane cytoskeleton linker ezrin is present in astrocytes (16–18). Ezrin regulates the structure and the function of specific domains of the plasma membrane (19, 20). It plays an important role in the assembly of epithelial microvilli; we therefore hypothesized that it might be involved in the formation of the PAP, which displays dimensions similar to those of epithelial microvilli.

Results

The PAPs are mostly submicroscopic structures. They appear as a diffuse background even at high magnification, and have thus been overlooked in a number of studies despite adequate markers. We performed double immunostaining of GFAP and ezrin in the CNS. We have applied subdiffraction microscopy by combining 1.4-NA lenses (plan-apochromat oil objective, 63× or 100×; Zeiss) with deconvolution (calibration information is provided in *Materials and Methods* and Fig. S1). Ezrin immunoreactivity was not present in identified glial GFAP-positive processes. Rather, GFAP and ezrin immunoreactivities were mutually exclusive (Fig. 1*A*, *1*), but the structures, when analyzed as high-magnification 3D reconstructions, were continuous at single points (Fig. 1*A*, *2*, and Movies S1 and S2). Ezrin-positive puncta were interconnected by minute structures, often at the detection threshold of the system, and organized as bushy complexes connected by a single stalk to the GFAP-positive glial stem processes (Fig. 1*A*, *2*, and Movies S1 and S2). We interpret the ezrin-positive structures as abundant PAPs, as PAPs are typically devoid of GFAP-positive glial filaments (21). Further, the expression of ezrin in brain is restricted to astrocytes (16) and ependymal cells (22), and a comparable organization of bushy complexes was observed in ultrastructural 3D reconstructions of (Bergmann) glial cells (23).

Given the restricted localization of ezrin in the extremely fine PAPs, we investigated the general significance of ezrin for PAP formation. When primary astrocytes were transfected with plasmids expressing ezrin siRNA and the EGFP reporter, the EGFP-positive cells displayed low ezrin immunoreactivity and significantly fewer filopodia in relation to neighboring, nontransfected cells or cells transfected with a control plasmid (Fig. 1*B*, *1* and *2* and Fig. S2).

We then examined to which extent PAP formation requires the regulated association of ezrin with the plasma membrane and the actin cytoskeleton. Ezrin interacts with membrane proteins through its N-terminal domain, and with F-actin through a C-terminal actin-binding site (19). This interaction requires an activation step that consists in the sequential binding of ezrin to

Author contributions: M.L., E.A., and A.D. designed research; M.L., G.A., F.P., and A.D. performed research; F.P. and M.A. contributed new reagents/analytic tools; M.L., G.A., E.A., and A.D. analyzed data; and M.L., M.A., and A.D. wrote the paper.

The authors declare no conflict of interest.

This article is a PNAS Direct Submission.

Freely available online through the PNAS open access option.

[1]To whom correspondence should be addressed. E-mail: derouiche@em.uni-frankfurt.de.

This article contains supporting information online at www.pnas.org/lookup/suppl/doi:10.1073/pnas.1100957108/-/DCSupplemental.

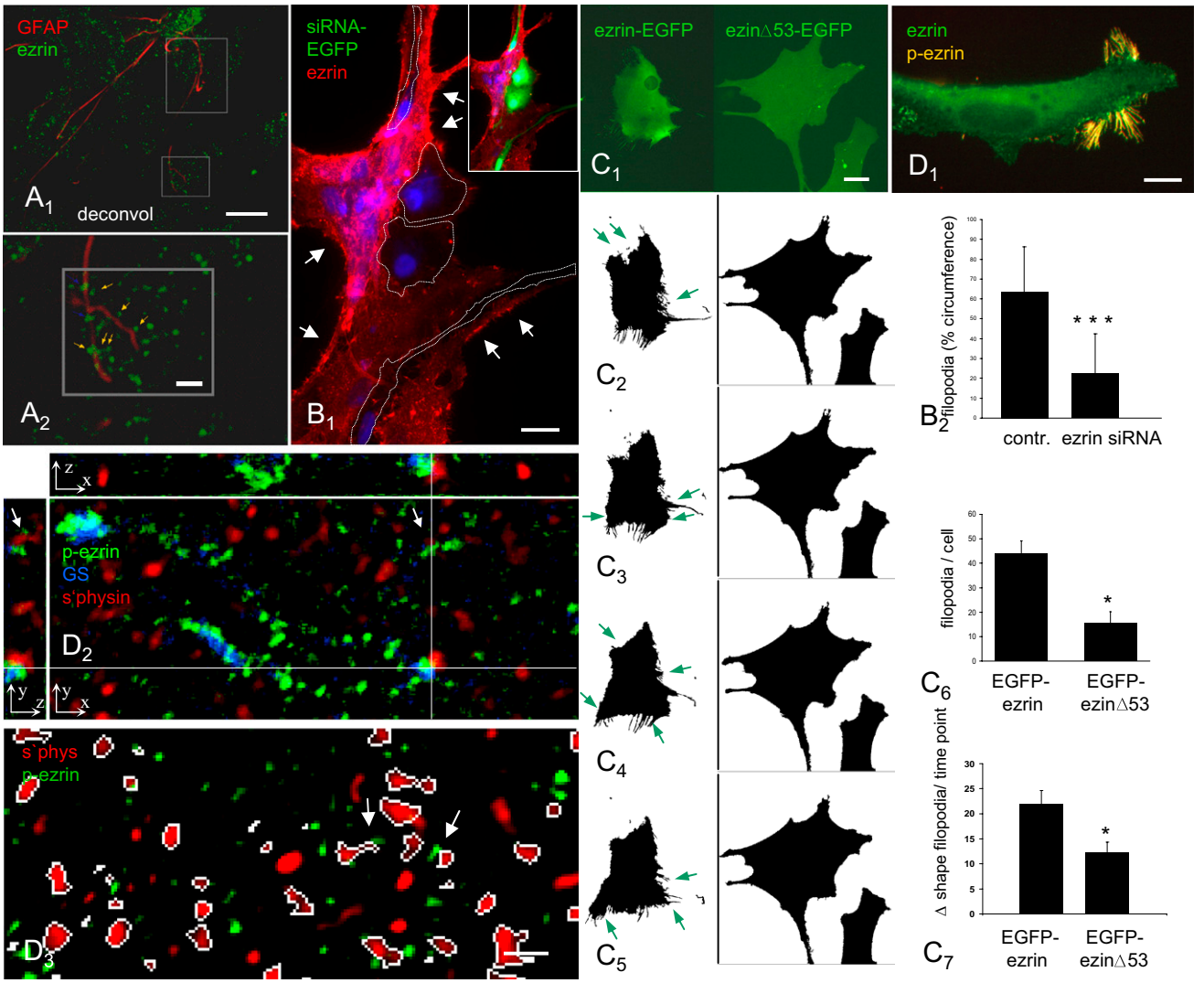

Fig. 1. Astrocytes in the CNS display two types of processes. (*A*) Double-labeled cryostat sections of rat hippocampus were investigated by epifluorescence microscopy with subsequent deconvolution. *1*, The GFAP-positive stem processes and discrete ezrin-positive puncta are mutually exclusive. *2*, Selected processes (boxed areas in *1*) magnified to the limit of light microscopic resolution, and the rotation of 3D reconstructions (Movies S1 and S2) reveal the structural continuity of the two structures (arrows mark points of continuity). (Scale bar: 1 μm.) (*B*) Ezrin is required for filopodia formation in primary astrocytes. *1*, Astrocytes transfected with an ezrin siRNA plasmid containing a CMV promotor-driven EGFP-cDNA (*Inset*, green; outlined in main figure) display diminished ezrin immunoreactivity (red channel) compared with neighboring, nontransfected cells. The processes and free cell boundaries of the transfected cells display fewer ezrin-immunoreactive filopodia, in comparison with other boundaries running parallel (arrows in *1*). Nuclei are stained blue. *2*, The extent of filopodia-covered cell circumference is significantly reduced in the siRNA-transfected cells ($n = 169$) in relation to the control plasmids ($n = 247$ cells; $P < 0{,}001$, Student's *t* test; mean ± SD). Fig. S2 compares the two individual siRNAs and three control plasmids. (*C*) Filopodia dynamics in primary astrocytes requires the membrane-to-cytoskeleton link by ezrin. *1*, *Left*: Ezrin–EGFP in primary astrocytes is predominantly localized to filopodia and microspikes. *1*, *2*, and *6*: Primary astrocytes transfected with ezrin–EGFP (*Left*, $n = 18$) display significantly more filopodia ($P < 0{,}05$, Mann–Whitney test) than those transfected with dominant-negative ezrinΔ53-EGFP (*Right*, $n = 13$). *1–5* and *7*: Thresholded live microscopy frames sampled at 30-min intervals show that cells expressing ezrin–EGFP ($n = 10$) are more motile, displaying significantly more ($P < 0.05$, Student's *t* test) shape changes per time point (green arrows in *2–5* and *7*) than cells expressing ezrinΔ53-EGFP ($n = 12$), which are relatively stationary (Movie S3). (*D*) The phosphorylated form of ezrin is selectively localized in the PAPs. *1*, Phospho-T567 ezrin, but not overall ezrin, is restricted to filopodia of fixed, cultured astrocytes. *2*, At higher magnification of hippocampal astrocytic processes in situ (overview shown in Fig. S3*A*), phospho-T657-ezrin–positive puncta are always associated with glial, GS-positive structures. Phospho-T657-ezrin immunoreactivity is often found in PAPs ensheathing axon terminals (*z*-views of hairline crossing and arrows). Perisynaptic astrocyte processes in situ consistently display activated ezrin. *3*, In rat hippocampal specimens (stratum radiatum, CA1), synapses or phospho-T657-ezrin-containing PAPs were defined as objects. The percentage of each object class contributing to glia–synaptic contact was determined. White outlines are around synapses which contact PAPs positive for phospho-T657-ezrin. In most cases, the contacts are obvious (arrows); if not, the corresponding PAP is in a different plane of section. Deconvolution, 0.1-μm optical section. (Scale bars: *A*, *1*, 5 μm; *A*, *2*, 1 μm; *B*, *1*, 2 μm, *C*, *1–5*, 15 μm, *D*, *1*, 15 μm; *x/y/z* arrows in *D*, *2* and *3*, 1 μm.)

PIP2 and phosphorylation of Thr567 present in the F-actin–binding site (24, 25). Normal ezrin–EGFP expressed in primary astrocytes was present at the plasma membrane and in the numerous filopodia (Fig. 1*C*, *1*, and arrows in Fig. 1*C*, *2–5*). In contrast, astrocytes displayed significantly less filopodia when transfected with a C-terminally truncated form of ezrin (ezinΔ53–EGFP) that can no longer interact with the actin cytoskeleton (26) (Fig. 1*C*, *6*, and compare left and right in Fig. 1*C*, *1–5*). This truncated protein was homogeneously distributed at the plasma membrane, yet it displayed a dominant-negative effect on filopodia formation (Fig. 1*C*, *1*). Further, the role of ezrin in structural plasticity was studied by live microscopy. Cultured astrocytes

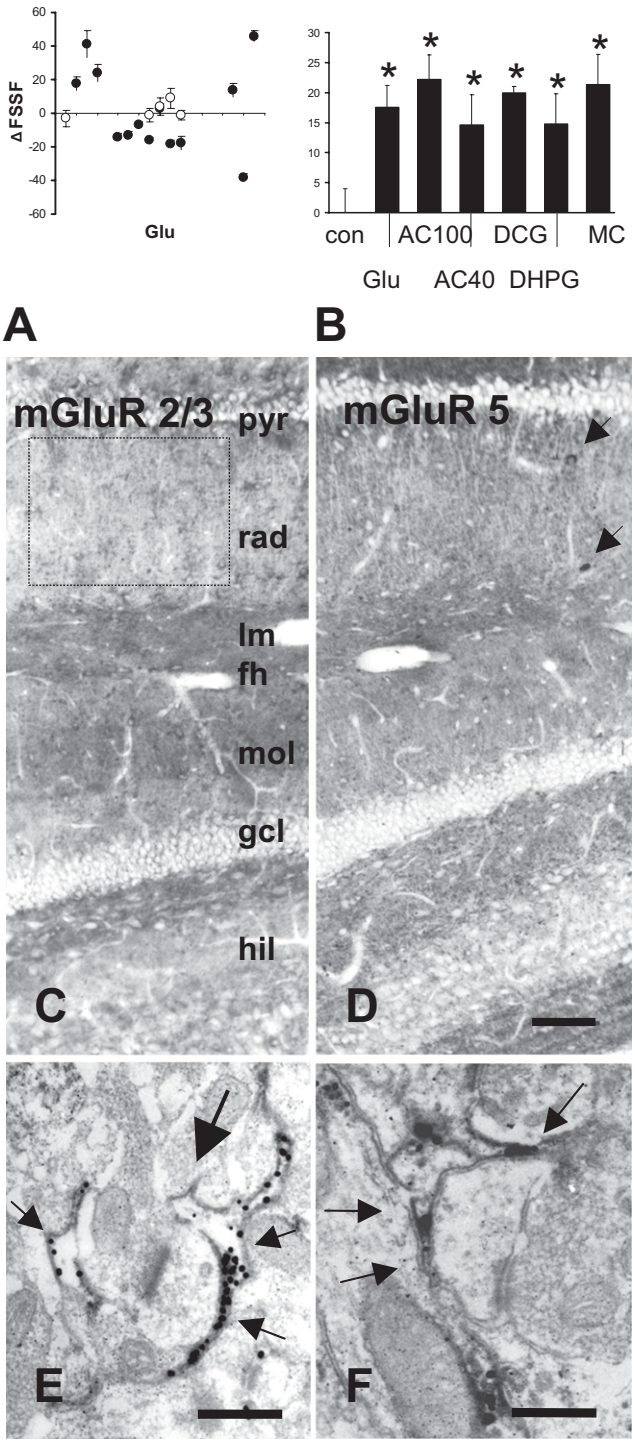

Fig. 2. Glutamate-induced filopodia motility in astrocytes is mediated by mGluRs 3 and 5. Primary astrocytes were incubated for 5 min with glutamate or glutamate analogues, then fixed and stained with anti-GFAP for cell identification, and with Oregon green–phalloidin for revealing the actin-containing filopodia (Fig. S4A). (*A*) Mean values from experiments on glutamate-induced filopodia dynamics show positive values for formation and negative ones for retraction. Filled circles are significantly different from control ($P < 0,05$, Student's *t* test). Each data point or bar in *A* or *B* includes filopodia measurements from 80 to 170 astrocytes. (*B*) The bars show the absolute values for the mGluR agonists and antagonists applied; all are significantly higher than control ($P < 0,05$, Student's *t* test). con, control; glu, glutamate; AC100, t-ACPD 100 μM; AC40, t-ACPD 40 μM; DCG, DCG IV; MC, MCCG I. mGluRs 3 and 5 are preferentially localized in the PAPs in vivo. (*C* and *D*) MGluR 2/3 and 5 labeling of astrocytes in rat hippocampus appears faintly diffuse or as fluffy patches (boxed area in *C*), in addition to interneurons (arrows in *D*). (*E* and *F*) The diffuse light microscopic staining (Fig. 2 *C* and *D*) is based on the abundance of submicroscopic glial processes at the ultrastructural level. The silver grains (silver-intensified DAB) can be seen in the extremely fine PAPs (<100 nm, small arrows in *E* and *F*) ensheathing the pre- and/or postsynaptic element (spine head in *E* and *F*), sometimes sealing the synaptic cleft (bold arrow in *E*). The systematic presence of both mGluRs in PAPs is shown in the overview of this motif (Figs. S5 and S6). (Scale bars: *C* and *D*, 100 μm; *E* and *F*, 0.5 μm.) pyr, stratum pyramidale; rad, radiatum; lm, lacunosum moleculare; fh, hippocampal fissure; mol, molecular layer; gcl, granule cell layer; hil, hilus.

can grow out short filopodia within less than 1 min (27). In astrocytes transfected with normal ezrin–EGFP, the ezrin-containing filopodia were highly dynamic (Fig. 1*C*, *1*–*5*) and ezrin was associated with membrane regions of high motility (Movie S3). Grouped puncta appearing and disappearing in the cell represent microspikes extending in the culture medium (Movie S3). In contrast, only small shape changes were observed in cells expressing ezrinΔ53–EGFP: they displayed very few short filopodia and microspikes (arrows in Fig. 1*C*, *1*–*5*), and were also less motile (Fig. 1*C*, *7*, and Movie S3). Transfections with ezrin siRNA or dominant-negative ezrin thus indicate that ezrin and its linker function are required for formation and motility of astrocytic filopodia.

As the phosphorylation of ezrin at T567 has been shown to occur only when ezrin is associated with the subplasmalemmal actin cytoskeleton (26), we examined the distribution of ezrin in astrocytes. Cultured astrocytes were double-stained for ezrin and phospho-T567 ezrin. The localization of ezrin phosphorylated at T567 was absolutely restricted to filopodia and microspikes (Fig. 1*D*, *1*). As an in vitro finding, substantial amounts of overall ezrin could also be seen diffusely throughout the cytoplasm (Fig. 1 *B*, *1*, and *D*, *1*), unlike astrocytes in situ, which are hardly recognizable in ezrin-stained brain sections (16) (Fig. 1*A*, *1*). The activated form of ezrin is thus restricted to membrane extensions further supporting a functional role of ezrin in filopodia formation. To transfer this finding to the in vivo situation, the rat hippocampus was triple-stained with antibodies directed against phospho-T567 ezrin, and glutamine synthetase (GS), an astrocytic marker that also reveals the PAPs, particularly around synapses (28). An anti-synaptophysin antibody was used to label the axon terminals. Phospho-T567 ezrin in the neuropil showed a punctate distribution, which did not outline obvious cellular structures but was clearly and consistently associated with identified, GS-positive profiles of astrocytes (Fig. S3*A*). Synaptophysin labeling did not coincide with that of phospho-T567 ezrin; instead, it was frequently juxtaposed to it (Fig. 1*D*, *2*). Quantitative analysis shows that nearly 58% of all synapses are touched by PAPs containing phospho-T567 ezrin (Fig. 1*D*, *3*, and Fig. S3*B*), which is comparable to the proportion of hippocampal synapses with glial contacts observed ultrastructurally (60–70%) (29). The minor discrepancy might be explained by limited detection of small amounts of phospho-T567 ezrin in the finest PAPs.

Next we investigated the regulation of PAP motility. Application of glutamate, the transmitter of most CNS synapses, to primary astrocytes seeded at low density induced elongation or retraction of filopodia along all directions (Fig. 2*A* and Fig. S4), as expected from previous studies (5, 6). The receptors mediating this process were investigated by the use of glutamate analogues (Fig. 2*B*). Trans-ACPD (40 or 100 μM), an agonist of group 1 and group 2 metabotropic glutamate receptors (mGluRs 1/5 and 2/3, respectively) (30), elicited responses analogous to those of glutamate, and the same was induced by DCGIV (100 μM), specific of group 2 mGluRs (30), and DHPG (100 μM), specific of group 1 mGluRs (30) (Fig. 2*B*). Combination of glutamate with MCCG I (400 or 800 μM), an mGluR 2 antagonist (30), left the responses unchanged. Taken together with previous molecular results that had excluded the presence of mGluRs 1 and 2 in astrocytes (31), our results suggest glutamate-induced motility of thin astrocyte processes to be mediated by activation of mGluR 3 or 5.

Expression of the latter receptors by glial cells in situ has not been systematically established (32, 33). By using silver intensification of DAB to detect the extremely small antigen quantities in structures as small as the PAPs (28), we observed a very similar, diffuse staining pattern for both mGluRs in the rat hippocampus (Fig. 2 *C* and *D*). This is the pattern characteristic of the selective labeling of the PAPs. At the ultrastructural level, the silver grains were systematically present in the fine PAPs (Fig. 2 *E* and *F* and Fig. S5 and S6), which collectively constitute the diffuse "background" (Fig. 2 *C* and *D*). The mGluR subtypes shown to mediate filopodia motility in vitro might therefore stimulate rapid PAP motility in the hippocampus as well, which is supported by the preferential PAP localization of these mGluRs. Importantly, the PAPs, although extremely thin, may also contain mitochondria localized in bulgings or branching points (Fig. S7).

We further tested in the hypothalamus of the intact animal whether a change in physiological, identified glutamatergic activity is paralleled with concomitant PAP changes, a prediction of glutamate-induced glial process motility. It is established that the synapses of the retinal ganglion cells projecting to the hamster suprachiasmatic nucleus (SCN) are glutamatergic and initiate photic synchronization of the circadian clock (34), so that their synaptic activity can be monitored over the light/dark (LD) cycle. Also, diffuse mGluR5 staining characteristic of PAPs coincides with the terminal field of the retinal projection to the SCN (Fig. S8). Anti-ezrin staining was applied to display the PAPs selectively (shown at high resolution in Fig. S9). Ezrin immunoreactivity in the SCN was compared in animals killed at two critical time points around the LD transition, Zeitgeber time (ZT) 10 (light, $n = 6$) or ZT14 (dark, $n = 7$). The significantly different levels of ezrin staining at ZT10 and ZT14 (Fig. 3) are consistent with rhythmic glutamate concentration in the SCN (35), in particular because ezrin staining was more intense at ZT14 when glutamate levels peak (35), in line with glutamate-induced PAP plasticity. Future biochemical and ultrastructural studies are, however, required to clarify whether increased ezrin immunoreactivity reflects ezrin protein synthesis at the onset of the night or differential ezrin availability for immunoreactivity staining based on sequestration or subcellular redistribution.

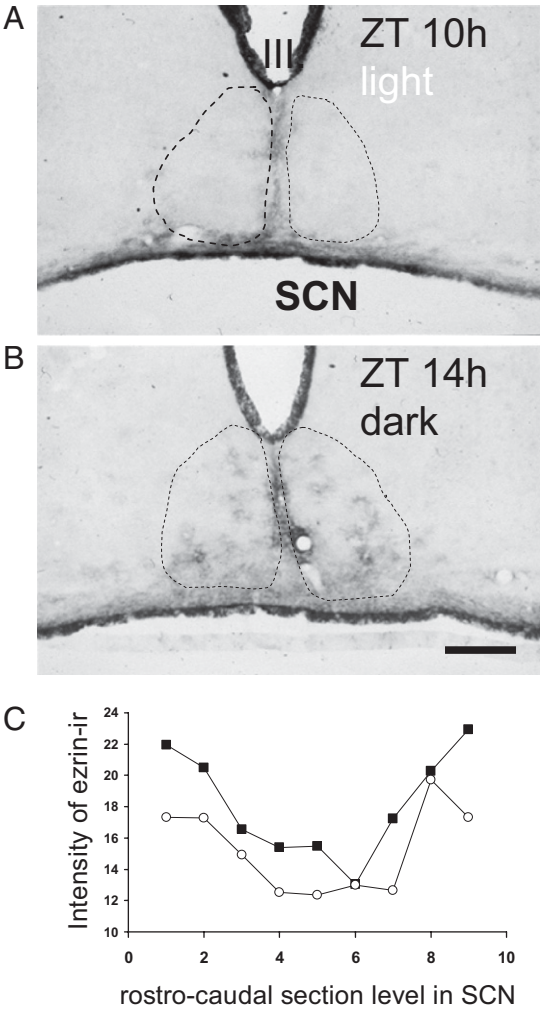

Fig. 3. Changes in the PAPs in vivo are in synchrony with changes in identified physiological glutamatergic activity. (*A* and *B*) Ezrin immunocytochemistry in hamster brain sections at the level of the SCN (dashed line). (*A*) Only the ependyma of the third ventricle (III.) and the midline tanycytes are labeled at 2 h before onset of the animal's nocturnal activity (ZT, 10 h). (*B*) Two hours after start of nocturnal activity (ZT, 14 h) in the dark, the PAPs in the SCN are selectively labeled in the characteristically diffuse pattern. (*C*) This effect is significant as quantified by densitometry ($P < 0{,}002$, paired Student's *t* test). Each data point represents the mean values from seven (ZT14, filled squares) or six animals (ZT10, open circles). The entire experiment was repeated twice with three or four animals per group, yielding similar and significant results. (Scale bars: 200 μm.)

Discussion

Altogether, the data show that the motility of astrocyte filopodia in vitro requires the membrane-cytoskeleton linker ezrin and that this motility can be induced by glutamate via mGluR3 and mGluR5 activation. We assume that the findings also apply to the in vivo situation. (*i*) The relevant proteins—ezrin and mGluRs 3 and 5—are present in and even preferentially targeted to the PAPs (in situ). (*ii*) Although there are no synapses in the cell culture studied, astrocyte filopodia and PAPs share some features relevant to motility. They are comparable in size and cytoskeletal equipment, being free from microtubules and intermediate filaments (21). Also, as actin is their only cytoskeletal component and only this can convey rapid (<1 min) shape changes, motility of filopodium and the PAP must be based on an actin mechanism (7), which is also rapid in vivo (6). (*iii*) As the perisynaptic glial sheath also displays the activated form of ezrin (Fig. 1*D*, *2* and *3*), this forms the basis of its well known plasticity. (*iv*) Activity changes of glutamatergic synapses in the behaving animal are in synchrony with changes in PAPs (Fig. 3). We suggest that synaptically released glutamate stimulates glial mGluRs on the nearby PAP, which leads to PAP elongation or retraction, a process involving intracellular mechanisms based on actin and ezrin. This would also require constant, energy-consuming actin remodeling. The presence of mitochondria in PAPs (Fig. S7) (36) is thus important because mitochondrially derived ATP helps to fuel actin assembly and disassembly, but also to control sodium and glutamate homeostasis in a small astrocytic compartment. In addition to providing ATP for GS—a key enzyme in the glutamate–glutamine shuttle—astrocytic mitochondria in PAPs may also directly participate in degradation of glutamate (37). As an example, the present in vitro evidence focuses on glutamate as the most abundant CNS transmitter, and astrocytes cultured from cortex. We assume that, in vivo, other transmitters are also operational, in addition to glutamate or in a region-dependent manner, as astrocytes display receptors for most transmitters. Also, a comparable influence of, for example, growth factors or cytokines on filopodia formation cannot be excluded.

The quantitative replication of glutamate effects by mGluR ligands suggests that glutamate-induced filopodia motility is solely mediated by mGluR activation. However, formation of the typically narrow and elongate PAP structure in Bergmann glia depends on Ca^{2+} influx through AMPA receptors (8, 15) not identified in hippocampal or cortical astrocytes (38). Here, mGluR-mediated intracellular PAP motility mechanisms might similarly work by an increase in intracellular Ca^{2+} concentration through release from intracellular stores triggered by direct and indirect mGluR3 or 5 signaling (30). Regarding the possibility of indirect, glutamate-

induced mechanisms, we can exclude factors released from neurons, which are absent in primary astrocyte culture. Autocrine effects cannot be strictly excluded, such as glutamate-induced astrocytic release of, for example, growth factors, cytokines, or small-molecule gliotransmitters (e.g., ATP). However, it appears unlikely that glial release of ATP or other substances would lead to effective medium concentrations (39, 40) in our model, in which astrocytes are deliberately cultured at high interindividual distance with 0.05 μL diffusion volume per cell.

The complementary staining pattern of GFAP and ezrin immunoreactivities in situ suggests that the glial stem processes and PAPs represent distinct cellular compartments. The PAP's particular morphofunctional properties are established by the specific targeting of ezrin and mGluRs 3 and 5, among other proteins, to the PAP (Figs. 1*A*, *1* and *2*, and 2 and Figs. S5 and S6): the PAP is extremely narrow (Fig. 2 *E* and *F*) (21), and only the PAP, but not the GFAP-positive stem process, is highly motile in vivo (6). By responding to glutamatergic activity, the PAP can also generate localized Ca^{2+} signals, which remain restricted to the "microdomain" (23) and do not spread to the parent stem process. However, it is unclear how these and other proteins are targeted to the PAP, whether they are transported as supramolecular aggregates, and how they are maintained within the PAP.

Materials and Methods

Primary astrocytes were prepared and enriched by the rotary shaker method (41) and replated in appropriate dishes at densities for subsequent immunostaining, transfection or filopodia measurements (*SI Materials and Methods*). Brain sections were obtained from rats perfusion-fixed with 4% paraformaldehyde (PFA; for light microscopy) or with 2% PFA and 2% glutaraldehyde (for EM) in phosphate buffer (PB). Primary antibodies applied in this study were mouse anti-ezrin (42, 1:1,000, 2 h, clone 3C12; Sigma), anti-GFAP linked to CY3 (1 h, 1:400, Sigma), rabbit anti–phospho-ezrin/radixin/moesin (for tissue sections; Cell Signaling Technology), mAb 297S (for cultured cells) (43) (gift of S. Tsukita, Kyoto University, Kyoto, Japan), mouse anti-GS (1:200; Chemicon), mouse anti-synaptophysin linked to oyster 656 (1:100; Synaptic Systems), rabbit-anti mGluR 2/3 (32) (1:500; Chemicon), and rabbit anti-mGluR 5 (33) (1:100; Chemicon). The detailed protocols for staining of cells and sections at the light microscopic or EM level are supplied in *SI Materials and Methods*. For ultrastructural visualization of the very low DAB signal even in the fine PAPs, which would normally not be detected, the chromogen DAB was further silver-enhanced (28). Filopodia were quantified by using the filopodia sensitive shape factor (FSSF), which represents a measure integrating length and number of the filopodia of a given cell independent of its overall shape and ramifications (*SI Materials and Methods*). For quantification of ezrin immunoreactivity in the SCN, hamsters were maintained under a 12/12 h LD cycle (*SI Materials and Methods*), and image processing and measurements were performed as previously described (44).

ACKNOWLEDGMENTS. We thank Dr. S. Tsukita for the generous gift of mAb 297S (CPERM), Dr. R. Lamb for supplying the EGFP plasmids, Dr. M. Thümmler for support in developing the automated filopodia measurements, and Dr. J. Walter for kind support with cell culture facility. The excellent technical assistance by S. Gaedicke, C. Papillon, B. Rost, and T. Schwalm is gratefully acknowledged. This project was promoted by the inspiring discussions with Dr. J. Wolff and Dr. M. Frotscher. This work was supported by Deutsche Forschungsgemeinschaft Grant DE 676.

1. Haydon PG, Carmignoto G (2006) Astrocyte control of synaptic transmission and neurovascular coupling. *Physiol Rev* 86:1009–1031.
2. Volterra A, Meldolesi J (2005) Astrocytes, from brain glue to communication elements: the revolution continues. *Nat Rev Neurosci* 6:626–640.
3. Chao TI, Rickmann M, Wolff JR (2002) *The Tripartite Synapse: Glia in Synaptic Transmission*, eds Volterra A, Magistretti P, Haydon P (Oxford Univ Press, Oxford), pp 3–23.
4. Eccles J, Ito M, Szentagothai J (1967) *The Cerebellum as a Neuronal Machine* (Springer, Berlin).
5. Hirrlinger J, Hülsmann S, Kirchhoff F (2004) Astroglial processes show spontaneous motility at active synaptic terminals in situ. *Eur J Neurosci* 20:2235–2239.
6. Haber M, Zhou L, Murai KK (2006) Cooperative astrocyte and dendritic spine dynamics at hippocampal excitatory synapses. *J Neurosci* 26:8881–8891.
7. Nishida H, Okabe S (2007) Direct astrocytic contacts regulate local maturation of dendritic spines. *J Neurosci* 27:331–340.
8. Iino M, et al. (2001) Glia-synapse interaction through Ca^{2+}-permeable AMPA receptors in Bergmann glia. *Science* 292:926–929.
9. Reichenbach A, Derouiche A, Kirchhoff F (2010) Morphology and dynamics of perisynaptic glia. *Brain Res Brain Res Rev* 63:11–25.
10. Lavialle M, Bègue A, Papillon C, Vilaplana J (2001) Modifications of retinal afferent activity induce changes in astroglial plasticity in the hamster circadian clock. *Glia* 34:88–100.
11. Oliet SHR, Piet R, Poulain DA, Theodosis DT (2004) Glial modulation of synaptic transmission: Insights from the supraoptic nucleus of the hypothalamus. *Glia* 47: 258–267.
12. Theodosis DT, Poulain DA (1993) Activity-dependent neuronal-glial and synaptic plasticity in the adult mammalian hypothalamus. *Neuroscience* 57:501–535.
13. Oliet SHR, Piet R, Poulain DA (2001) Control of glutamate clearance and synaptic efficacy by glial coverage of neurons. *Science* 292:923–926.
14. Theodosis DT, Poulain DA, Oliet SH (2008) Activity-dependent structural and functional plasticity of astrocyte-neuron interactions. *Physiol Rev* 88:983–1008.
15. Hoogland TM, et al. (2009) Radially expanding transglial calcium waves in the intact cerebellum. *Proc Natl Acad Sci USA* 106:3496–3501.
16. Derouiche A, Frotscher M (2001) Peripheral astrocyte processes: Monitoring by selective immunostaining for the actin-binding ERM proteins. *Glia* 36:330–341.
17. Geiger KD, Stoldt P, Schlote W, Derouiche A (2000) Ezrin immunoreactivity is associated with increasing malignancy of astrocytic tumors but is absent in oligodendrogliomas. *Am J Pathol* 157:1785–1793.
18. Grönholm M, et al. (2005) Characterization of the NF2 protein merlin and the ERM protein ezrin in human, rat, and mouse central nervous system. *Mol Cell Neurosci* 28: 683–693.
19. Bretscher A, Edwards K, Fehon RG (2002) ERM proteins and merlin: Integrators at the cell cortex. *Nat Rev Mol Cell Biol* 3:586–599.
20. Gautreau A, Louvard D, Arpin M (2002) ERM proteins and NF2 tumor suppressor: the Yin and Yang of cortical actin organization and cell growth signaling. *Curr Opin Cell Biol* 14:104–109.
21. Peters A, Palay SL, Webster HdeF (1991) *The Fine Structure of the Nervous System: The Neurons and Supporting Cells.* (Oxford Univ Press, Oxford), 3rd ed.
22. Berryman M, Franck Z, Bretscher A (1993) Ezrin is concentrated in the apical microvilli of a wide variety of epithelial cells whereas moesin is found primarily in endothelial cells. *J Cell Sci* 105:1025–1043.
23. Grosche J, et al. (1999) Microdomains for neuron-glia interaction: Parallel fiber signaling to Bergmann glial cells. *Nat Neurosci* 2:139–143.
24. Fievet BT, et al. (2004) Phosphoinositide binding and phosphorylation act sequentially in the activation mechanism of ezrin. *J Cell Biol* 164:653–659.
25. Tsukita S, Yonemura S, Tsukita S (1997) ERM proteins: Head-to-tail regulation of actin-plasma membrane interaction. *Trends Biochem Sci* 22:53–58.
26. Coscoy S, et al. (2002) Molecular analysis of microscopic ezrin dynamics by two-photon FRAP. *Proc Natl Acad Sci USA* 99:12813–12818.
27. Cornell-Bell AH, Thomas PG, Smith SJ (1990) The excitatory neurotransmitter glutamate causes filopodia formation in cultured hippocampal astrocytes. *Glia* 3:322–334.
28. Derouiche A, Frotscher M (1991) Astroglial processes around identified glutamatergic synapses contain glutamine synthetase: Evidence for transmitter degradation. *Brain Res* 552:346–350.
29. Spacek J (1985) Three-dimensional analysis of dendritic spines. III. Glial sheath. *Anat Embryol (Berl)* 171:245–252.
30. Schoepp DD, Jane DE, Monn JA (1999) Pharmacological agents acting at subtypes of metabotropic glutamate receptors. *Neuropharmacology* 38:1431–1476.
31. Condorelli DF, et al. (1999) Expression and functional analysis of glutamate receptors in glial cells. *The Functional Roles of Glial Cells in Health and Disease*, eds Matsas R, Tsacopoulos M (Kluwer, Dordrecht, The Netherlands), pp 49–67.
32. Petralia RS, Wang YX, Niedzielski AS, Wenthold RJ (1996) The metabotropic glutamate receptors, mGluR2 and mGluR3, show unique postsynaptic, presynaptic and glial localizations. *Neuroscience* 71:949–976.
33. Romano C, et al. (1995) Distribution of metabotropic glutamate receptor mGluR5 immunoreactivity in rat brain. *J Comp Neurol* 355:455–469.
34. Ebling FJ (1996) The role of glutamate in the photic regulation of the suprachiasmatic nucleus. *Prog Neurobiol* 50:109–132.
35. Glass JD, Hauser UE, Randolph WW (1993) In vivo microdialysis of 5-hydroxyindoleacetic acid and glutamic acid in the hamster suprachiasmatic nuclei. *Am Zool* 33:212–218.
36. Lovatt D, et al. (2007) The transcriptome and metabolic gene signature of protoplasmic astrocytes in the adult murine cortex. *J Neurosci* 27:12255–12266.
37. Pardo B, et al. (2011) Brain glutamine synthesis requires neuronal-born aspartate as amino donor for glial glutamate formation. *J Cereb Blood Flow Metab* 31:90–101.
38. Seifert G, Steinhäuser C (2001) Ionotropic glutamate receptors in astrocytes. *Prog Brain Res* 132:287–299.
39. Gourine AV, et al. (2010) Astrocytes control breathing through pH-dependent release of ATP. *Science* 329:571–575.
40. Shigetomi E, Kracun S, Sofroniew MV, Khakh BS (2010) A genetically targeted optical sensor to monitor calcium signals in astrocyte processes. *Nat Neurosci* 13:759–766.
41. McCarthy KD, de Vellis J (1980) Preparation of separate astroglial and oligodendroglial cell cultures from rat cerebral tissue. *J Cell Biol* 85:890–902.
42. Böhling T, et al. (1996) Ezrin expression in stromal cells of capillary hemangioblastoma. An immunohistochemical survey of brain tumors. *Am J Pathol* 148:367–373.
43. Matsui T, et al. (1998) Rho-kinase phosphorylates COOH-terminal threonines of ezrin/radixin/moesin (ERM) proteins and regulates their head-to-tail association. *J Cell Biol* 140:647–657.
44. Vilaplana J, Lavialle M (1999) A method to quantify glial fibrillary acidic protein immunoreactivity on the suprachiasmatic nucleus. *J Neurosci Methods* 88:181–187.